revista principia

ISSN 2447-9187

https://doi.org/10.18265/2447-9187a2025id8871

ORIGINAL ARTICLE

SUBMITTED January 30, 2025

APPROVED May 18, 2025

PUBLISHED ONLINE June 9, 2025

FINAL FORMATTED VERSION March 16, 2026

ASSOCIATE EDITOR
Dr. José Carlos de Lima Júnior

Increasing the bending strength of hardened AISI 1045 steel by milling processs

Ueliton Carvalho Alves [1] *

Gian Narciso de Oliveira Remundini [2]

Carlos Eiji Hirata Ventura [3]

[1] ueliton.alves@ifsp.edu.br
Federal Institute of Education, Science and Technology of São Paulo (IFSP), Piracicaba, São Paulo, Brazil

[2] gianremundini@gmail.com
São Carlos School of Engineering, University of São Paulo (USP), São Carlos, São Paulo, Brazil

[3] ventura@ufscar.br
Department of Mechanical Engineering, Federal University of São Carlos (UFSCar), São Carlos, São Paulo, Brazil

* *Corresponding author.*

ABSTRACT: Surface characteristics play a critical role in the initiation and propagation of defects in metallic components subjected to static or dynamic loading, thereby directly influencing mechanical performance and service life. Therefore, selecting an appropriate finishing process is essential for improving surface integrity and mechanical resistance. This study investigates the effects of cutting speed and feed per tooth on the flexural strength of AISI 1045 steel specimens subjected to hard machining using an 80 mm diameter end mill, with cutting speeds of 100 m/min and 400 m/min. Specifically, it evaluates the influence of surface roughness and the resulting changes in surface hardness on the bending behavior of the material. The findings indicate that surface roughness has a more pronounced effect on bending strength than the metallurgical alterations induced by the machining process. A reduction in maximum surface roughness from 4.66 µm to 3.02 µm – approximately 35% – resulted in a 51% increase in rupture stress and a 137% increase in deflection at fracture. In contrast, variations in surface hardness induced by machining were found to have a negligible effect on mechanical strength. Once failure is initiated, the material's hardness becomes even less relevant, as it does not influence crack propagation. These results highlight the importance of optimizing surface finishing parameters to improve the structural performance of hardened steels, particularly in the metalworking and automotive industries, where mechanical reliability and durability are paramount.

Keywords: flexural strength; hard machining; mechanical property; surface integrity; three-point bending test.

Aumento da resistência à flexão do aço AISI 1045 endurecido por processo de fresamento

RESUMO: *As características da superfície desempenham um papel crítico na iniciação e na propagação de defeitos quando componentes metálicos são submetidos a cargas estáticas ou dinâmicas, influenciando diretamente seu desempenho mecânico e sua vida útil. Portanto, a seleção de um processo de acabamento apropriado é essencial para melhorar a*

integridade da superfície e a resistência mecânica. Este estudo investiga os efeitos da velocidade de corte e do avanço por dente na resistência à flexão de corpos de prova de aço AISI 1045 submetidos à usinagem dura usando uma fresa de topo de 80 mm de diâmetro, com velocidades de corte de 100 m/min e 400 m/min. Especificamente, ele avalia a influência da rugosidade da superfície e das mudanças resultantes na dureza da superfície no comportamento de flexão do material. Os resultados indicam que a rugosidade superficial tem um efeito mais pronunciado na resistência à flexão do que as alterações metalúrgicas induzidas pelo processo de usinagem. Uma redução na rugosidade máxima da superfície de 4,66 µm para 3,02 µm – aproximadamente 35% – resultou em um aumento de 51% na tensão de ruptura e num aumento de 137% na deflexão na fratura. Em contraste, verificou-se que as variações na dureza superficial induzidas pela usinagem têm um efeito insignificante na resistência mecânica. Uma vez iniciada a falha, a dureza do material torna-se ainda menos relevante, pois não influencia a propagação de trincas. Esses resultados destacam a importância da otimização dos parâmetros de acabamento superficial para melhorar o desempenho estrutural de aços endurecidos, particularmente nas indústrias metalúrgica e automotiva, nas quais a confiabilidade mecânica e a durabilidade são cruciais.

Palavras-chave: *ensaio de flexão em três pontos; integridade superficial; propriedades mecânicas; resistência à flexão; usinagem de dureza.*

1 Introduction

Surface integrity plays a crucial role in extending the service life of engineering components by influencing properties such as corrosion, wear, and fatigue resistance (Zheng *et al*., 2020). Consequently, numerous studies have examined the effects of machining processes on surface characteristics (Li; Guan; Zhao, 2018; Nguyen, 2019; Patel; Gandhi, 2019; Perez *et al*., 2018; Tomadi *et al*., 2017). These characteristics include surface topography (e.g., defects and roughness), microstructure (e.g., grain size and texture), and mechanical properties (e.g., hardness and residual stresses), all of which are governed by the cutting parameters employed during machining (Liang; Liu; Wang, 2019).

This is particularly relevant in the context of hard machining, a process that is increasingly adopted as an alternative to grinding for finishing operations. Hard machining offers advantages such as greater geometric flexibility, elimination of cutting fluids, and reduction of the manufacturing process chain. However, the machinability of hardened steels is inherently limited due to the high forces, stresses, and temperatures developed at the cutting edge of the tool (Sales *et al*., 2020). The intense plastic deformation and thermo-mechanical loads involved in the cutting process can lead to surface modifications through metallurgical transformations (Jamshidi; Mejías; Ghadbeigi, 2023).

According to Castanhera and Diniz (2016) and Kumar, Singh, and Kalsi (2017), milling of hardened steels can yield high-quality surface finishes, potentially eliminating the need for secondary processes such as polishing in the fabrication of molds and dies. Studies by Hassanpour *et al*. (2016) and Das, Panda, and Dhupal (2017) reported that increasing cutting speed and decreasing feed per tooth lead to reductions

in surface roughness, with feed per tooth being the most critical parameter. Pereira, Rodrigues, and Abrão (2017) observed that elevated values of cutting speed and feed per tooth were associated with the formation of untempered martensite, which results in increased microhardness. From tensile testing, Frodal *et al*. (2020) observed that plastic anisotropy caused by aggressive machining conditions can induce surface hardening, thereby affecting ductile fracture behavior.

In addition to roughness and hardness, cutting conditions also influence the residual stress state of machined surfaces. Compressive residual stresses, often observed at lower cutting speeds, are typically induced by plastic deformation and microstructural changes. Conversely, high cutting speeds and feed rates tend to generate tensile residual stresses due to increased thermal effects (Fangyuan *et al*., 2019; Zhou *et al*., 2024). In a study by Huang *et al*. (2018), three-point bending fatigue tests revealed that milled bars exhibited an 83% longer fatigue life than polished ones, attributed to the higher compressive residual stresses and enhanced microhardness induced by the milling process. Similarly, significant correlations between cutting conditions and fatigue limits were identified by Bertolini *et al*. (2025) for Ti-6Al-4V and by Tan *et al*. (2020) for TC17 titanium alloy. Conversely, Li *et al*. (2025) found that milling and grinding operations on GH4169 nickel alloy resulted in reduced fatigue resistance when surface roughness increased, even when applying different machining techniques.

Although static mechanical tests are less frequently used to study the effects of surface integrity, static bending tests are particularly valuable for assessing the strength of hardened materials. These tests enable comparison of surface characteristics with fracture limits under quasi-brittle failure conditions. Additionally, they replicate service-like stress states by introducing both tensile and compressive stresses simultaneously (Gere; Timoshenko, 2001). Bending tests are especially beneficial for characterizing small or thin specimens, where conventional tensile testing may be impractical, according to ASTM C1161 (ASTM, 2018). For example, Izotov *et al*. (2009) demonstrated that grain refinement in pearlitic steels enhances strength and toughness under plastic deformation. Furthermore, due to their sensitivity to surface and subsurface defects, bending tests are widely employed in the evaluation of ceramics and composites, where surface integrity is crucial to performance (Callister; Rethwisch, 2020). In a foundational study, Molchanov (1976) assessed fracture energy under bending loads for various alloy steels, concluding that fracture exhibited quasi-static characteristics at high energy levels and fatigue-like behavior at lower energies.

Several studies have also addressed the impact of surface roughness on the formability of materials during bending. Wechsuwanmanee *et al*. (2021) observed that high roughness impairs cold formability by introducing geometric discontinuities that act as initiation sites for localized damage. Similarly, Münstermann *et al*. (2019) reported crack formation during bending of specimens with rougher surfaces.

Given the simplicity and sensitivity of bending tests in capturing the influence of surface integrity on the mechanical behavior of hardened steels, and the potential for process optimization through appropriate machining strategies, this study aims to explore the effect of surface roughness, produced by milling under varying cutting conditions, on the maximum load and deflection at rupture in three-point bending tests of AISI 1045 steel specimens. Improving mechanical performance through surface finish optimization may allow for the reduction of component cross-sections during the design phase, thus lowering material consumption and manufacturing costs. AISI 1045 steel was selected as the work material due to its widespread industrial use, which combines low cost, high machinability, and balanced mechanical

properties. This steel is commonly used in producing components such as front axle beams, shafts, leaf spring bearings, machine tool parts, and gears, making it particularly relevant for studies aimed at enhancing manufacturing efficiency and mechanical reliability.

Despite a substantial body of research on the influence of machining parameters on surface integrity, particularly concerning fatigue performance and wear resistance, there remains a noticeable gap in the literature regarding the impact of surface characteristics on the static mechanical behavior of hardened steels under quasi-brittle fracture conditions. Most existing studies emphasize fatigue life, residual stresses, or dynamic loading scenarios, with limited attention to static loading conditions, which are also critical for components subjected to high-strength but low-cycle demands. Furthermore, studies specifically linking surface roughness to bending strength and fracture deflection are scarce, particularly for medium-carbon steels such as AISI 1045 processed by hard machining. In this context, the present study distinguishes itself by systematically evaluating how surface roughness, controlled through variations in cutting speed and feed per tooth during milling, affects the flexural strength and ductility of hardened AISI 1045 steel. This approach not only deepens the understanding of the relationship between surface finish and structural performance but also offers practical insights for optimizing machining parameters to enhance mechanical reliability in applications where static strength is a critical design factor.

The remainder of this paper is organized into three sections: Section 2 describes the machining conditions, surface characterization procedures, and bending tests; Section 3 presents the effects of cutting parameters on surface integrity and mechanical performance; and Section 4 summarizes the key findings and practical implications.

2 Experimental procedure

Specimens of AISI 1045 steel, by ASTM A576-17 (ASTM, 2017a), with dimensions of 23 mm × 205 mm × 10 mm, were cut from sheets using a shear machine along the rolling direction to ensure uniform material properties and minimize variability caused by material inconsistencies. The specimens were then heat-treated according to the ABNT NBR NM 136 standard (ABNT, 2000). For the quenching process, they were heated in a muffle furnace (model ML-1400) at 825 °C for 25 minutes and subsequently cooled in water. For tempering, the specimens were reheated to 150 °C for 2 hours and allowed to cool to room temperature. This thermal treatment resulted in an average hardness of 705.65 ± 53.74 HV.

Subsequently, the specimens were machined on an automatic milling machine (Clever PBM-4VS) with a maximum power of 4 kW and a maximum spindle speed of 4,200 rpm. The machine was equipped with an end mill (Korloy RM16 ACN6080HR-M), 80 mm in diameter with six teeth. The cutting inserts (Korloy ONMX-MM) used were made of cemented tungsten carbide (ISO grade P40) and coated with TiN via physical vapor deposition (PVD).

After heat treatment, a 1 mm surface layer was removed from each specimen (Figure 1a) under defined cutting conditions of speed and feed per tooth (Table 1). A constant depth of cut of 0.25 mm was maintained throughout the experiments, and four passes were performed to finish each surface. The tool was symmetrically aligned over the workpiece to maintain an approximately constant chip thickness

ISSN 2447-9187

Figure 1 ▼
(a) Specimen dimensions before and after milling.
(b) Tool positioning relative to the workpiece surface.
Source: prepared by the authors

along the machined surfaces and minimize variations in mechanical and thermal loading (Figure 1b).

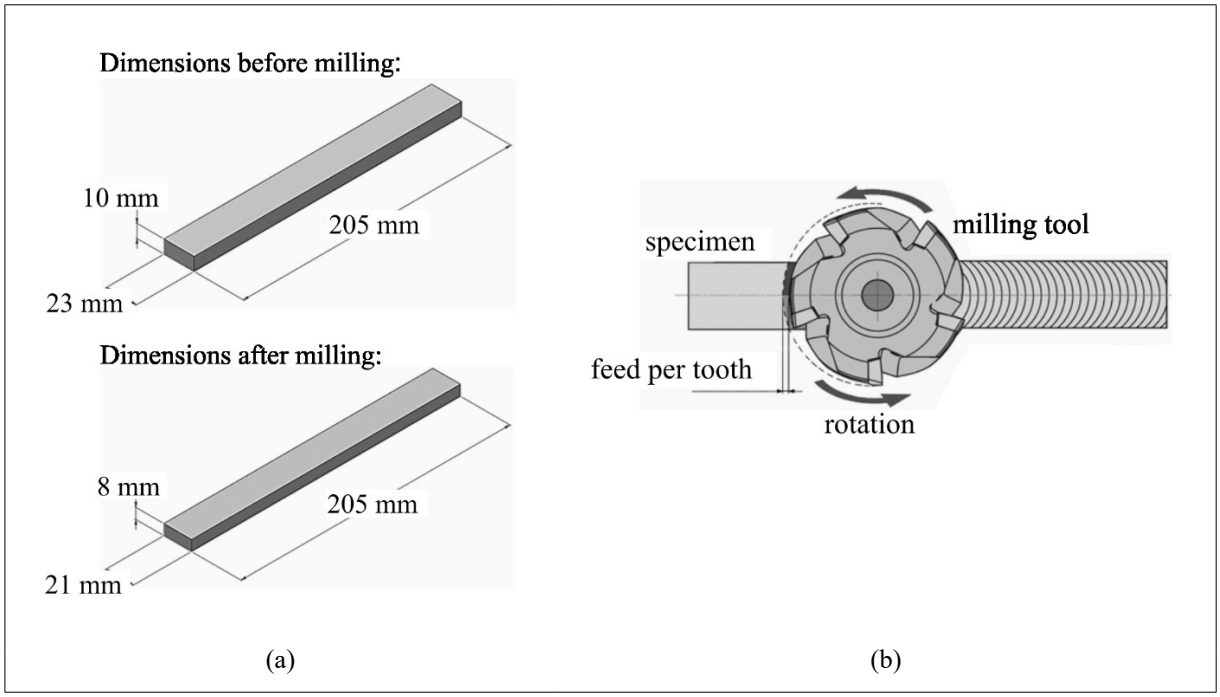

Table 1 ▶
Applied cutting conditions.
Source: research data

Experiment	Cutting speed v_c (m/min)	Feed per tooth f_z (mm)
1	100	0.05
2		0.10
3		0.24
4		0.44
5	400	0.01
6		0.05
7		0.10

Surface roughness was measured at the center of two specimens by acquiring 500 profiles in the feed direction (Figure 2) using a confocal microscope (Alicona InfiniteFocus SL) connected to a personal computer with Alicona Metrology Measurement software for image processing. To obtain a comprehensive characterization of the surface topography, the following roughness parameters were analyzed: *Rz* (mean of five peak-to-valley heights), *Rp* (maximum peak height), *Rv* (maximum valley depth), *Rsk* (skewness), and *Rku* (kurtosis). These parameters are relevant due to their influence on the mechanical behavior of specimens during bending tests by introducing potential stress concentration sites. *Rz* provides an overall roughness description, while *Rp* and *Rv* individually describe peak and valley characteristics. *Rsk* indicates the asymmetry of the roughness profile (*Rsk* < 0 suggests wide peaks and sharp valleys; *Rsk* > 0 implies

sharp peaks and wide valleys), and *Rku* describes profile peakedness (*Rku* > 3 indicates sharp peaks and valleys; *Rku* < 3 indicates broader features).

Figure 2 ▶
Roughness profile measurement method.
Source: prepared by the authors

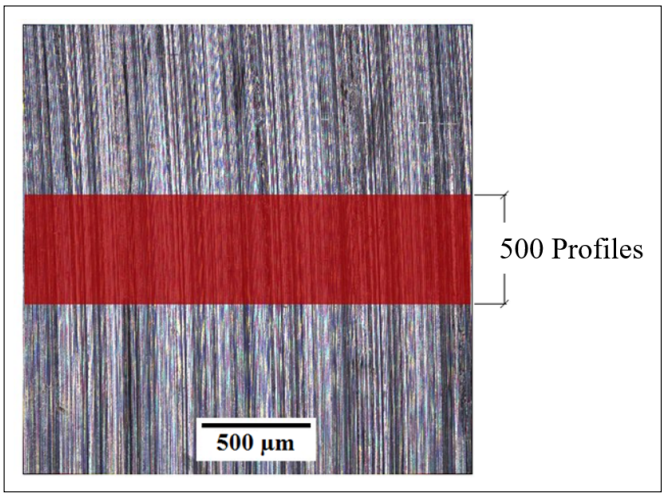

To evaluate potential metallurgical alterations caused by machining, Vickers hardness was measured before and after machining on two specimens from each cutting condition using a Future-Tech FM-800 microdurometer. The test applied a 500 gf load for 15 seconds, following ASTM E384-17 (ASTM, 2017b). Five measurements were taken per specimen, and the average and standard deviation of the ten measurements in total were used in the analysis.

Subsequently, the machined specimens underwent three-point bending tests using a universal testing machine (Jinan Liangong CMT-100), which has a load capacity of 110 kN, a maximum opening of 400 mm, and anvils and supports with radii of 8 mm (Figure 3).

Figure 3 ▶
Schematic representation of the three-point bending test.
Source: prepared by the authors

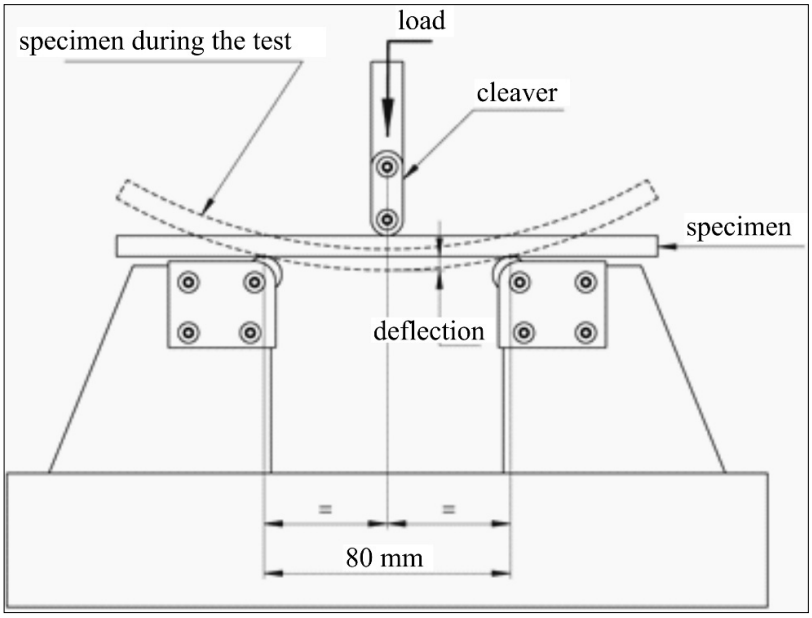

The maximum loads (P_{max}) obtained during testing, together with the geometric parameters of the specimens, were used to calculate the rupture stress, as expressed in Equation 1. This stress value was then correlated with the measured surface roughness parameters and the deflection at failure. Equation 1, as defined

by ASTM E855-08 (ASTM, 2013) for the bending test of flat metallic specimens under static loading, incorporates the following variables:

$$\sigma_{rup} = \frac{1.5 \times P_{max} \times L}{b \times h^2} \quad (1)$$

where b = specimen width (= 21 mm), h = specimen thickness (= 8 mm), and L = distance between the support and the load application point (= 40 mm).

Finally, post-test fracture characteristics were documented using a DNT DigiMicro Profi digital microscope with up to 300× magnification.

3 Results and discussion

Section 3 is further divided into two subsections. Subsection 3.1 details the surface characterization, including roughness and hardness measurements under various machining conditions. Subsection 3.2 discusses the influence of these surface characteristics on flexural strength and provides an analysis of the fracture behavior of the specimens.

3.1 Surface characterization

The amplitude parameters of the surface roughness profile are presented in Figure 4. The progressive increase in Rz with higher feed per tooth values (f_z) (Figure 4a) is closely associated with the kinematics of the milling process, in which each cutting insert follows a circular trajectory while the tool advances linearly. The magnitude of the resulting surface irregularities is related to peaks and valleys formed primarily due to material deformation and removal, respectively.

Figure 4 ▼
Evolution of amplitude roughness parameters as a function of cutting speed (v_c) and feed per tooth (f_z): (a) *Rz*, (b) *Rp*, and (c) *Rv*.
Source: research data

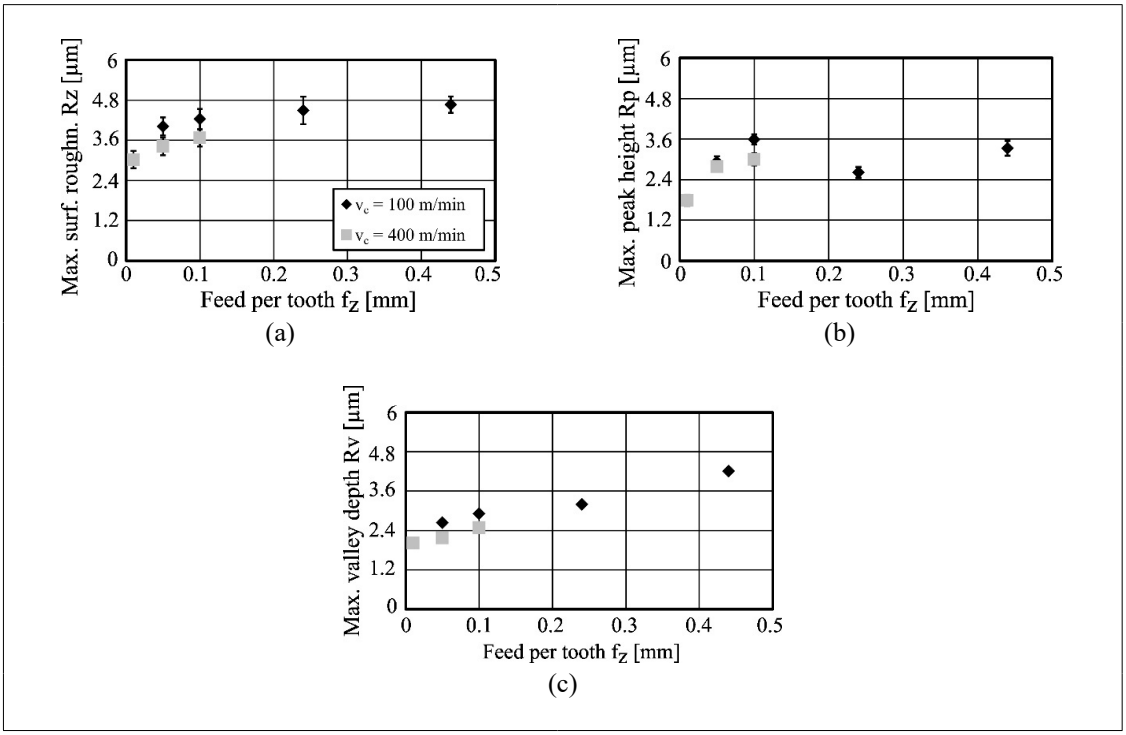

Material deformation exhibits a non-systematic behavior, as the hardened material tends to fracture before undergoing significant plastic deformation. This explains the oscillatory pattern observed in the *Rp* values, despite a general upward trend with increasing feed (Figure 4b). In contrast, material removal occurs more uniformly, becoming the dominant factor influencing surface roughness formation. This is corroborated by the behavior of *Rv* (Figure 4c), which closely resembles that of *Rz*, indicating that valleys are more consistently influenced by the cutting parameters and are more significant than peaks in the assessment of roughness in milled surfaces.

Conversely, higher cutting speeds tend to result in lower roughness values, which is typically attributed to a reduction in material strength due to elevated temperatures, thereby facilitating chip removal. Bensouilah *et al*. (2016), in a turning process, reported a decrease in Ra as cutting speed increased from 75 m/min to 200 m/min on AISI D3 steel (63 HRC), using mixed alumina inserts (CC6050) with TiN coating in an SNGA 120408 T01525 (ISO) tool, and mixed ceramic inserts (CC650) in an SNGA 120408 T01020 (ISO) tool. Similarly, Gaitonde *et al*. (2016) observed a reduction in surface roughness in the milling of annealed AISI D2 steel (255 HB) with increasing cutting speed from 90 m/min to 150 m/min. However, further increases to 180 m/min resulted in a deterioration of surface finish.

Figure 5 ▼
Behavior of roughness profile distribution parameters as a function of cutting speed (v_c) and feed per tooth (f_z): (a) skewness (*Rsk*), (b) kurtosis (*Rku*).
Source: research data

Figure 5 presents the profile distribution parameters under the tested conditions. No clear trend is observed for skewness (*Rsk*, Figure 5a), which shows average values near zero with high dispersion, suggesting a relatively symmetrical distribution of peaks and valleys and no systematic influence from the machining parameters. Regarding kurtosis (*Rku*, Figure 5b), although no direct correlation with cutting parameters is identified, the measured values generally exceed 3, indicating the presence of sharp peaks and valleys across all tested conditions.

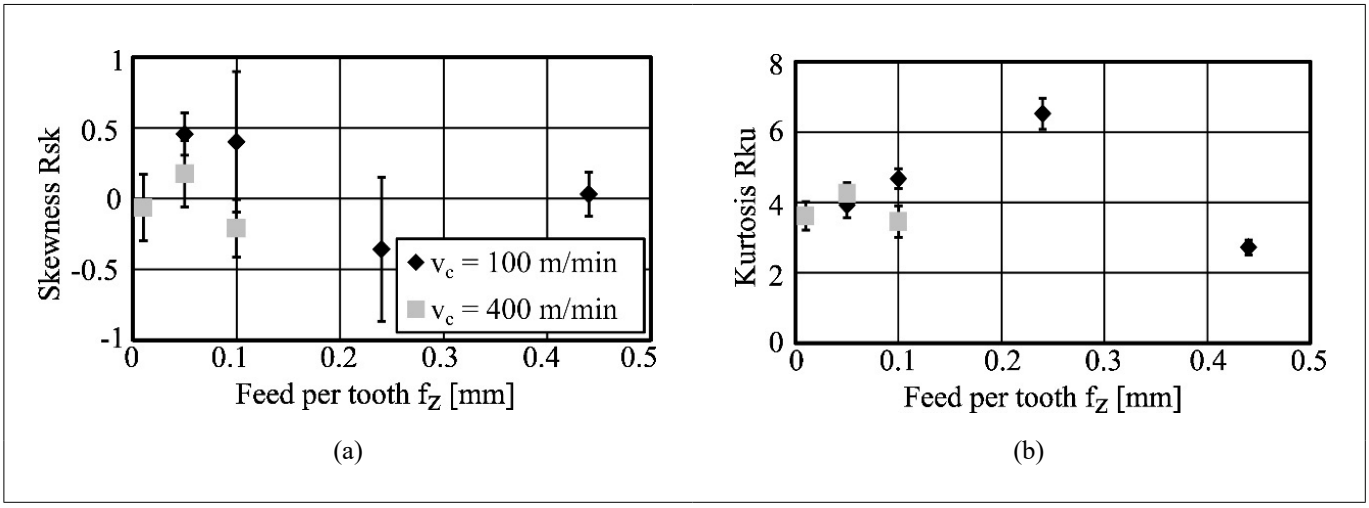

Surface roughness and hardness were both affected by the machining process, as illustrated in Figure 6, which shows the variation in hardness (ΔHV) before and after milling. Positive values indicate that the material was harder before machining, suggesting surface softening induced by the process. Although more pronounced softening (i.e., higher ΔHV) is generally observed at higher feeds per tooth and lower cutting speeds, the considerable data scatter and relatively small changes (ranging from 2 to 9 HV) limit the possibility of drawing definitive conclusions regarding the influence of cutting parameters on surface hardness.

ISSN 2447-9187

Figure 6 ▶
Surface hardness variation (ΔHV) of specimens machined under different cutting conditions.
Source: research data

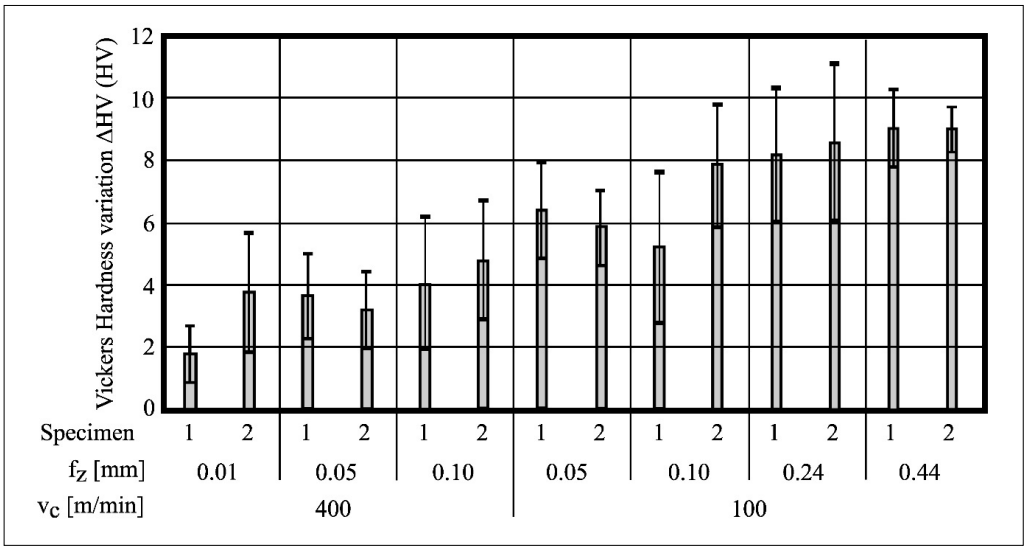

In contrast, Hassanpour *et al*. (2016), while machining 4340 alloy steel (450 HV), observed a hardness increase attributed to the elimination of the plowing effect, which can induce anisotropic plastic flow and elevate surface hardness.

Table 2 ▼
Average values of maximum surface roughness, hardness variation, and results from the three-point bending tests under different cutting conditions.
Source: research data

3.2 Influence of surface characteristics on flexural strength and fracture analysis

Table 2 presents the average values for stress and deflection at rupture obtained from the three-point bending tests. It is observed that higher feeds per tooth and lower cutting speeds correlate with reduced strength parameters.

Cutting speed (v_c) (m/min)	Feed per tooth (f_z) (mm)	Maximum roughness (Rz) (µm)	Hardness variation (ΔHV) (HV)	Stress at rupture (σ_{rup}) (MPa)	Deflection at rupture (δ_{rup}) (mm)
100	0.05	4.02	7.48	2.68	5.56
	0.10	4.24	8.20	2.35	4.31
	0.24	4.49	8.53	2.14	4.29
	0.44	4.66	8.71	2.09	3.75
400	0.01	3.02	2.07	3.15	8.88
	0.05	3.42	3.40	2.93	7.90
	0.10	3.67	4.07	2.61	5.52

Given that roughness and hardness were affected differently by the machining process, the most statistically significant factor influencing material strength should be identified. Figures 7a and 7b illustrate Pareto charts showing the influence of maximum surface roughness (Rz) and hardness variation (ΔHV) on stress (σrup) and deflection (δ_{rup}) at rupture, respectively, using a 95% confidence interval ($\alpha = 0.05$). For both output variables, surface roughness was more influential, while hardness variation did not significantly affect flexural strength.

ISSN 2447-9187

Figure 7 ▶
Pareto chart showing the influence of maximum roughness *Rz* and hardness variation *ΔHV* on (a) stress σ_{rup} and (b) deflection δ_{rup} at rupture.
Source: research data

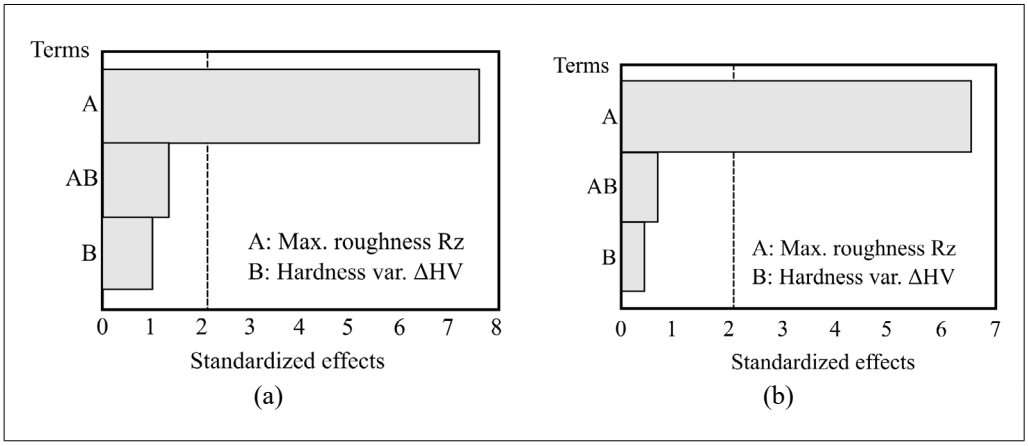

Figure 8 ▼
Representative curves of the load (*P*) versus deflection (δ) for three specimens (1, 2, and 3) machined at v_c = 100 m/min and f_z = 0.44 mm.
Source: research data

This predominant effect of surface roughness on flexural strength is attributed to crack initiation at surface defects, which act as stress concentrators and serve as the primary failure mechanism. The variation in surface hardness does not significantly alter material strength, and its influence diminishes further after crack initiation, as it does not affect crack propagation. Despite the material's high hardness, elastic and plastic deformation zones still form (Figure 8), although insufficient to notably reduce the cross-sectional area and, consequently, load-bearing capacity. However, Li *et al*. (2025) observed that increased microhardness can positively influence fatigue resistance by hindering crack initiation and propagation.

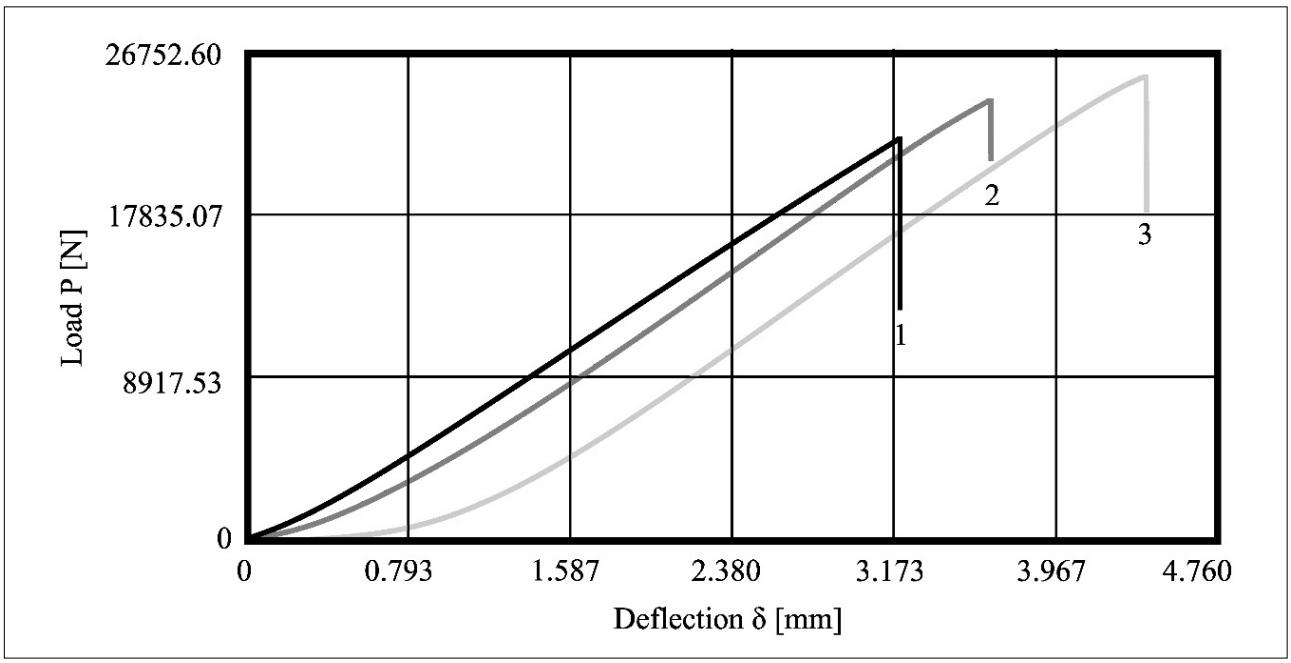

Based on these findings, a least squares method was employed to stablish correlations between surface roughness with strength parameters (Figure 9). A power function yielded correlation coefficients exceeding 90% in both cases.

ISSN 2447-9187

Figure 9 ▶
Correlation of (a) stress σ_{rup} and (b) deflection δ_{rup} at rupture with maximum surface roughness *Rz*.
Source: research data

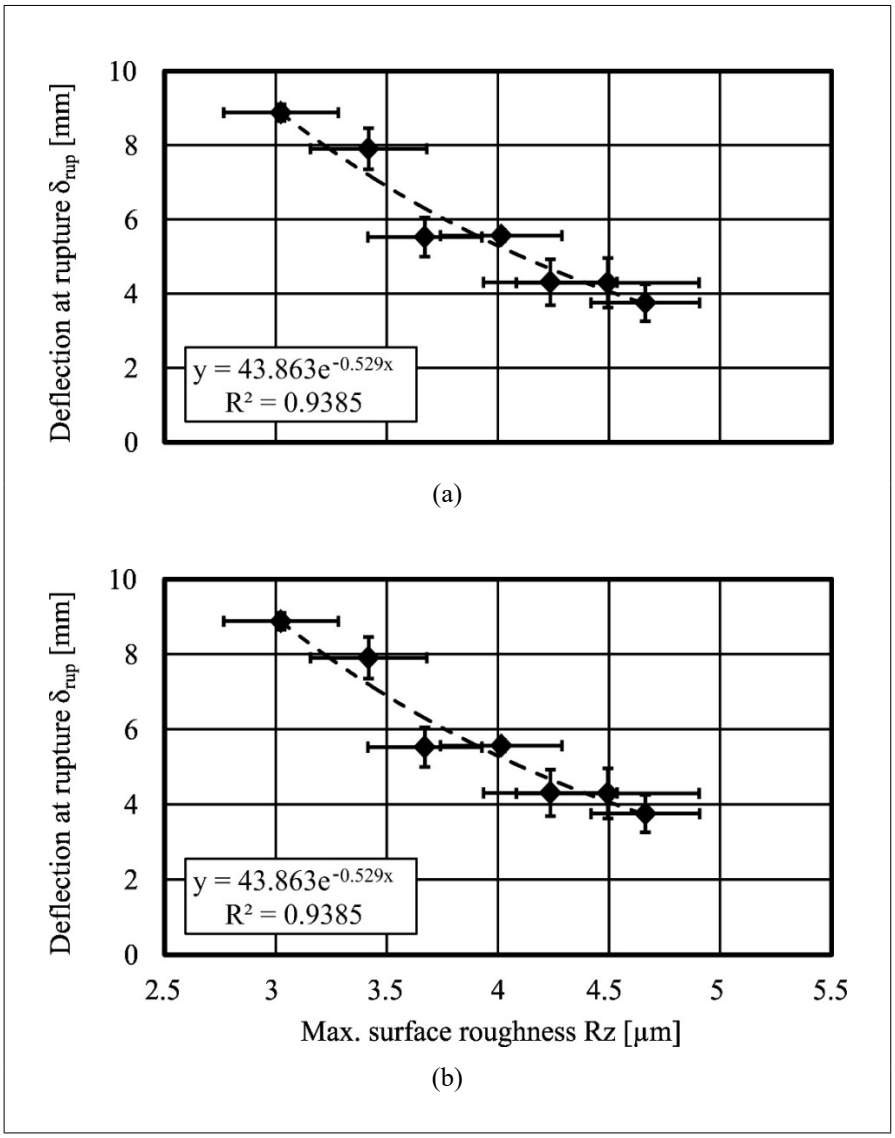

An increase in *Rz* corresponds to a greater peak-to-valley distance, which promotes the formation of stress concentration sites and may ultimately lead to fracture. Given that different machining processes can produce similar *Rz* values while generating distinct surface topographies in terms of peak heights and valley depths, it becomes necessary to determine which specific features better correlate with the investigated strength parameters.

Using the same regression method, weak correlations were observed for *Rp* (R^2 = 40.80% for σ_{rup} and R^2 = 56.04% for δ_{rup}) as illustrated in Figures 10a and 10b. By contrast, stronger correlation coefficients were obtained for *Rv* (R^2 = 83.34% for σ_{rup} and R^2 = 77.94% for δ_{rup}), according to Figures 10c and 10d. These findings suggest that crack initiation predominantly occurs at valley bottoms.

The results indicate that both stress and deflection at rupture decrease as the maximum valley depth (*Rv*) increases, a condition directly influenced by higher feed per tooth and lower cutting speed (v_c = 100 m/min). This correlation demonstrates that machining parameters resulting in increased surface roughness significantly impair the flexural strength and ductility of the material.

ISSN 2447-9187

Figure 10 ▶
Correlation between (a) stress σ_{rup} and (b) deflection δ_{rup} at rupture with maximum peak height *Rp*, and between (c) stress σ_{rup} and (d) deflection δ_{rup} at rupture with maximum valley depth *Rv*.
Source: research data

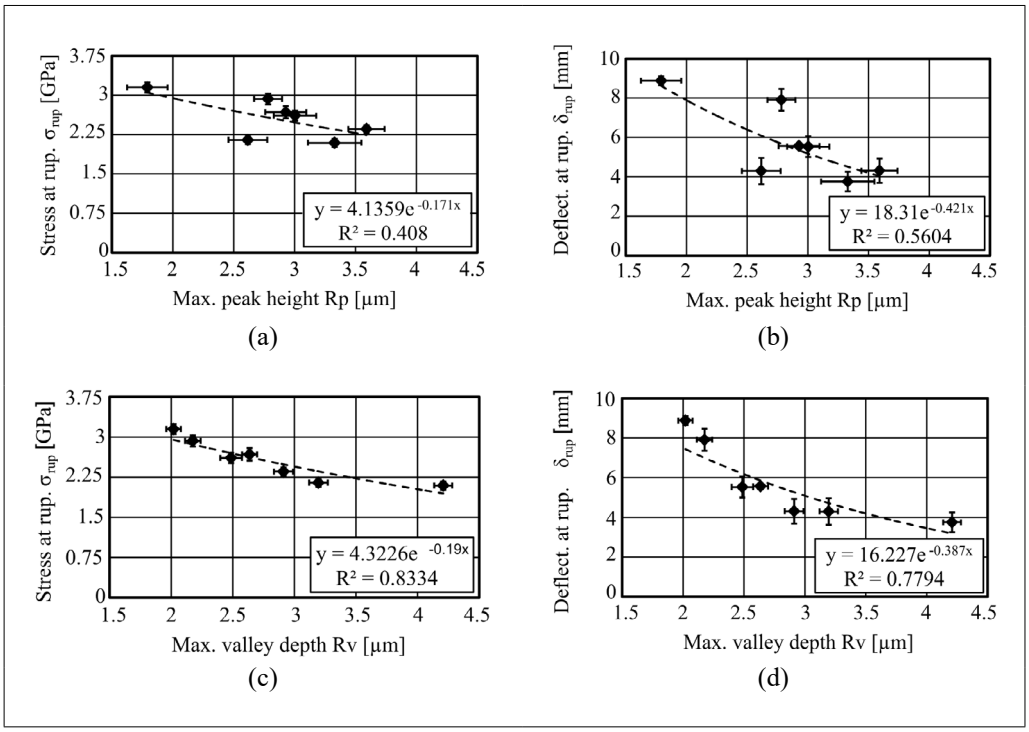

Lee, Lee, and Park (2023) reported that stress concentrations induced by surface roughness are mainly influenced by the morphology of valleys aligned with the loading direction. In particular, deeper and narrower valleys promote higher localized stress concentrations. Consistent with these findings, Li *et al*. (2025), investigating the fatigue performance of milled Ti-6Al-4V surfaces, concluded that stress concentration at the valley notches of chatter marks significantly contributes to the reduction of fatigue life.

The analysis indicates that shallower valleys in the roughness profile require higher stresses and deflections to induce failure in components subjected to bending loads. Therefore, optimizing surface finish during design can reduce component cross-section and weight, leading to lower material usage. For instance, a 100% reduction in valley depth (from ~4.2 µm to ~2.1 µm) results in a 50% increase in the stress required for rupture (from ~2.1 GPa to ~3.1 GPa). Considering a rectangular cross-section and applying Equation 1, this allows for a 33% reduction in component width (or an 18% reduction in thickness).

Arola and Williams (2002) demonstrated that the effective stress concentration factor increased with surface roughness in AISI 4130 CR steel plates, resulting in a significant reduction in high-cycle fatigue strength due to intensified localized stresses and facilitated crack initiation. This effect is particularly critical in components subjected to cyclic loading, where surface imperfections act as micro-notches accelerating fatigue damage.

Coto *et al*. (2011) reported that increased feed rates generate greater heat during cutting, resulting in higher tensile residual stresses. Conversely, higher cutting speeds promote a more adiabatic process with reduced heat dissipation through the chip, leading to lower tensile stresses. Maximum stress was found to localize around 30° from the cutting direction.

The failure mode of specimens subjected to bending tests remained consistent under varying cutting parameters. A representative specimen is therefore presented for discussion. The macroscopic fracture surface (Figure 11a) exhibits a fibrous

ISSN 2447-9187

texture with several cavities, indicating plastic deformation preceding failure. Fracture initiated at the bottom surface, which was subjected to tensile stresses, and is characteristic of dimple rupture, occurring via microvoid nucleation and coalescence under tensile loading (Mode I, as defined by Kerlins (1987)).

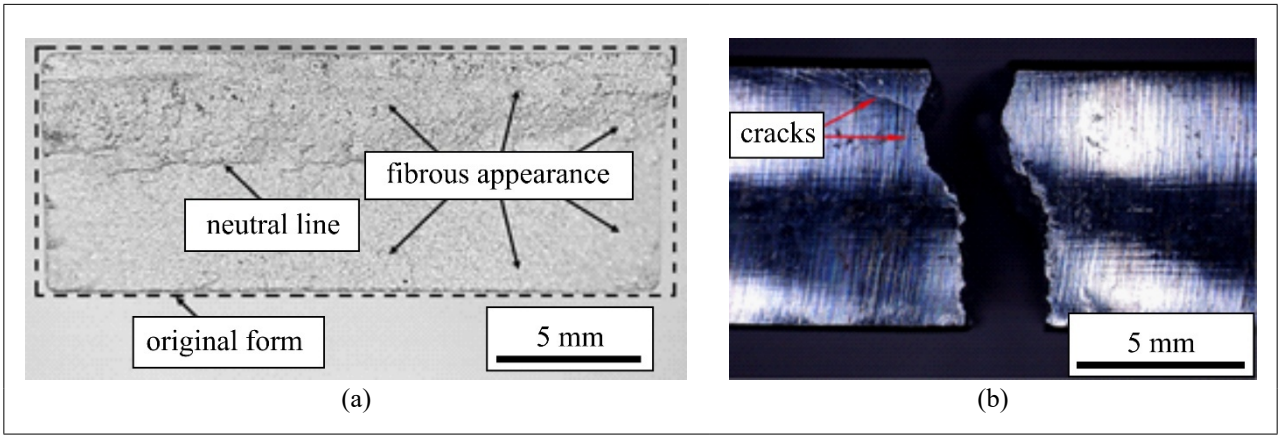

Figure 11 ▼
Cross-section and side view of a fractured specimen (v_c = 100 m/min, f_z = 0.05 mm). (a) Macroscope view of the fractured region. (b) Lateral view of fractured area.
Source: research data

The neutral axis, where compressive and tensile stresses are null and shear stress is at its maximum, is visible. Deformation of the original rectangular cross-section (shown as a dashed outline) is frequently observed in bent specimens that underwent plastic deformation before fracture. During bending, tensile and compressive stresses develop primarily along the longitudinal axis, with tensile stresses concentrated on the outer surface and compressive stresses on the inner surface of the specimen (Singh; Kim; Choi, 2019). Unlike uniaxial tests, bending imposes both stress types simultaneously, generating a more complex distribution that better simulates service conditions in structural components.

The lateral view (Figure 11b) shows that the fracture may initiate slightly away from the punch position, likely due to uncontrolled stress concentrations caused by surface irregularities. Subsurface cracking beneath the punch contact area was also observed. This phenomenon is consistent with Hertzian contact theory, which predicts a semi-elliptical pressure distribution for a plane-cylinder system, with maximum pressure and plastic yielding occurring beneath the surface (Williams; Dwyer-Joyce, 2001). These cracks converge near the workpiece midsection, where shear stress is at its highest.

Liu, Schraknepper, and Bergs (2022) demonstrated a clear relationship between surface roughness, residual stress, and cutting speed, key factors for ensuring the surface integrity of machined components. Increasing cutting speed (from 133 m/min to 160 m/min) tends to improve surface finish while also increasing thermal loads, thereby inducing tensile residual stresses during milling. Conversely, lower cutting speeds result in rougher surfaces but lead to more compressive residual stresses due to enhanced plastic deformation in the surface layer.

Zhao *et al*. (2024) identified multiple factors contributing to enhanced fatigue life following ultrasonic surface rolling. Among them, surface roughness was found to have the most significant impact on crack initiation resistance. However, excessive ultrasonic treatment may lead to premature crack propagation by degrading surface quality.

Li, Guo, and Guo (2013) examined dry milling of hardened AISI H13 steel molds (50 HRC) and concluded that high surface integrity can be maintained until flank wear reaches 0.2 mm. Surface roughness was found to depend on the combined effects of feed rate and radial depth of cut, with wear within this range not contributing significantly to increased roughness.

Lu *et al*. (2019), studying the milling of Inconel 718, found that cutting speed has the greatest effect on workpiece microhardness, followed by machining depth and feed per tooth. To minimize surface microhardness, a combination of higher cutting speed, lower feed per tooth, and shallower machining depth is recommended.

In summary, surface roughness and residual stresses are critical to the mechanical performance and structural integrity of machined parts. Improved surface finish, typically obtained via higher cutting speeds or post-processing techniques, delays crack initiation and extends fatigue life, but often introduces detrimental tensile residual stresses due to thermal effects. In contrast, conditions that promote compressive residual stresses (e.g., lower speeds or controlled deformation) may compromise surface quality but improve crack resistance. Achieving a balance between low surface roughness and favorable residual stress distribution is therefore essential for maximizing both performance and service life of components under mechanical loading.

Future investigations may include fractographic analysis using scanning electron microscopy, offering detailed insights into the underlying failure mechanisms. Fatigue testing also represents a promising method for validating the influence of surface roughness and microhardness under cyclic loading conditions. Additionally, numerical simulations could serve as a valuable tool for enhancing the understanding of the observed phenomena; however, at present, no suitable reference model or initial framework is available for their development. These complementary methodologies would enable a more comprehensive evaluation of the mechanical behaviour of components, thereby extending the findings of this study to more complex and realistic operational conditions.

4 Conclusions

Specimens of hardened AISI 1045 steel were machined under varying cutting conditions, and their surfaces were characterized by roughness and hardness measurements, and were subsequently subjected to three-point bending tests. The resulting mechanical performance and surface characteristics were subsequently analyzed and statistically correlated. Based on these findings, the following conclusions are drawn:

- The surface topography of a machined component is the primary factor influencing its flexural strength, particularly the stress and maximum deflection at rupture observed in bending tests. Valleys in the roughness profile exert a greater influence on mechanical performance than peaks, as cracks tend to initiate at stress concentration points associated with these valleys. This effect remains predominant throughout the entire roughness range analyzed, although the data suggest that when the *Rv* value is below approximately 2.5 µm, its impact on mechanical integrity becomes less significant;
- Within the tested range of machining parameters, potential metallurgical alterations at the surface, indicated by localized softening and variations in hardness, do not significantly affect the mechanical strength of the material;
- From a practical standpoint, a 100% reduction in valley depth may lead to a 50% increase in the stress required to induce rupture. In milling operations, such

improvement can be achieved by increasing the cutting speed and reducing the feed per tooth;

- Fractographic analysis indicated that machining conditions did not influence the fracture mechanism. All tested specimens exhibited ductile fracture characterized by microvoid nucleation and coalescence, which is typical of dimple rupture under tensile stress conditions.

It is recommended that cyclic fatigue tests be conducted to investigate the influence of surface roughness profiles on the number of cycles to crack initiation and propagation, thereby advancing the understanding of fatigue behavior under dynamic loading. Furthermore, additional tests, such as impact resistance or fracture under combined loading conditions, represent pertinent areas for future research and may provide a more accurate representation of service conditions.

Funding

The authors gratefully acknowledge the financial support provided by the Coordenação de Aperfeiçoamento de Pessoal de Nível Superior, Brasil (CAPES, Finance Code 001) and the São Paulo Research Foundation (Fundação de Amparo à Pesquisa do Estado de São Paulo – FAPESP, grant number 2017/12309-7).

Declaration of conflicting interests

The authors declare that there is no conflict of interest.

Author contribution

VENTURA, C. E. H.: conceptualization or design of the study/research; data analysis and/or interpretation. **RAMUNDINI, G. N. O.:** conceptualization or design of the study/research; data analysis and/or interpretation. **ALVES, U. C.:** data analysis and/or interpretation; final review with critical and intellectual contribution to the manuscript. All authors contributed to the writing, discussion, reading, and approval of the final version of the manuscript.

References

ABNT – ASSOCIAÇÃO BRASILEIRA DE NORMAS TÉCNICAS. **ABNT NBR NM 136**: Tratamentos térmicos de aço – Terminologia e definições. Rio de Janeiro: ABNT, 2000. In Portuguese.

AROLA, D.; WILLIAMS, C. L. Estimating the fatigue stress concentration factor of machined surfaces. **International Journal of Fatigue**, v. 24, n. 9, p. 923-930, 2002. DOI: https://doi.org/10.1016/S0142-1123(02)00012-9.

ASTM – AMERICAN SOCIETY FOR TESTING AND MATERIALS. **ASTM A576–17**: Standard specification for steel bars, carbon, hot-wrought, special quality. West Conshohocken: ASTM International, 2017a.

ASTM – AMERICAN SOCIETY FOR TESTING AND MATERIALS. **ASTM C1161**: Standard test method for flexural strength of advanced ceramics at ambient temperature. West Conshohocken: ASTM International, 2018.

ASTM – AMERICAN SOCIETY FOR TESTING AND MATERIALS. **ASTM E384-17**: Standard test method for microindentation hardness of materials. West Conshohocken: ASTM International, 2017b.

ASTM – AMERICAN SOCIETY FOR TESTING AND MATERIALS. **ASTM E855-08**: Standard test methods for bend testing of metallic flat materials for spring applications involving static loading. ASTM International, 2013.

BENSOUILAH, H.; AOUICI, H.; MEDDOUR, I.; YALLESE, M. A.; MABROUKI, T.; GIRARDIN, F. Performance of coated and uncoated mixed ceramic tools in hard turning process. **Measurement: Journal of the International Measurement Confederation**, v. 82, p. 1-18, 2016. DOI: https://doi.org/10.1016/j.measurement.2015.11.042.

BERTOLINI, R.; STRAMARE, A.; BRUSCHI, S.; GHIOTTI, A.; CAMPAGNOLO, A. Impact of cryogenic machining on the fatigue strength and surface integrity of wrought Ti6Al4V with equiaxed microstructure. **Engineering Failure Analysis**, v. 170, 109274, 2025. DOI: https://doi.org/10.1016/j.engfailanal.2025.109274.

CALLISTER, W. D.; RETHWISCH, D. G. **Materials Science and Engineering**: an introduction. 10. ed. Hoboken: Wiley, 2020.

CASTANHERA, I. C.; DINIZ, A. E. High speed milling of hardened steel convex surface. **Procedia Manufacturing**, v. 5, p. 220-231, 2016. DOI: https://doi.org/10.1016/j.promfg.2016.08.020.

COTO, B.; NAVAS, V. G.; GONZALO, O.; ARANZABE, A.; SANZ, C. Influences of turning parameters in surface residual stresses in AISI 4340 steel. **The International Journal of Advanced Manufacturing Technology**, v. 53, p. 911-919, 2011. DOI: https://doi.org/10.1007/s00170-010-2890-1.

DAS, S. R.; PANDA, A.; DHUPAL, D. Experimental investigation of surface roughness, flank wear, chip morphology and cost estimation during machining of hardened AISI 4340 steel with coated carbide insert. **Mechanics of Advanced Materials and Modern Processes**, v. 3, 9, 2017. DOI: https://doi.org/10.1186/s40759-017-0025-1.

FANGYUAN, Z.; CHUNZHENG, D.; WEI, S.; KANG, J. Effects of cutting conditions on the microstructure and residual stress of white and dark layers in cutting hardened steel. **Journal of Materials Processing Technology**, v. 266, p. 599-611, 2019. DOI: https://doi.org/10.1016/j.jmatprotec.2018.11.038.

FRODAL, B. H.; MORIN, D.; BORVIK, T.; HOPPERSTAD, O. S. On the effect of plastic anisotropy, strength and work hardening on the tensile ductility of aluminum alloys. **International Journal of Solids and Structures**, v. 188-189, p. 118-132, 2020. DOI: https://doi.org/10.1016/j.ijsolstr.2019.10.003.

GAITONDE, V. N.; KARNIK, S. R.; MACIEL, C. H. A.; RUBIO, J. C. C.; ABRÃO, A. M. Machinability evaluation in hard milling of AISI D2 steel. **Materials Research**, v. 19, n. 2, p. 360-369, 2016. DOI: https://doi.org/10.1590/1980-5373-MR-2015-0263.

GERE, J. M.; TIMOSHENKO, S. P. **Mechanics of materials**. 5. ed. Boston: PWS Publishing, 2001.

HASSANPOUR, H.; SADEGHI, M. H.; RASTI, A.; SHAJARI, S. Investigation of surface roughness, microhardness, and white layer thickness in hard milling of AISI 4340 using minimum quantity lubrication. **Journal of Cleaner Production**, v. 120, p. 124-134, 2016. DOI: https://doi.org/10.1016/j.jclepro.2015.12.091.

HUANG, W.; ZHAO, J.; NIU, J.; WANG, G.; CHENG, R. Comparison in surface integrity and fatigue performance for hardened steel ball-end milled with different milling speeds. **Procedia CIRP**, v. 71, p. 267-271, 2018. DOI: https://doi.org/10.1016/j.procir.2018.05.059.

IZOTOV, V. I.; GETMANOVA, M. E.; BURZHANOV, A. A.; KIREEVA, E. Y.; FILIPPOV, G. A. Effect of the pearlitic steel structure on the mechanical properties and fracture upon loading by static bending. **The Physics of Metals and Metallography**, v. 108, p. 606-615, 2009. DOI: https://doi.org/10.1134/S0031918X09120126.

JAMSHIDI, H.; MEJÍAS, F. C.; GHADBEIGI, H. A finite element assessment of the workpiece plastic deformation in machining of Ti-6Al-4V. **Procedia CIRP**, v. 117, p. 62-67, 2023. DOI: https://doi.org/10.1016/j.procir.2023.03.012.

KERLINS, V. Modes of fracture. *In*: ASM INTERNATIONAL. **ASM Handbook**: v. 12 –Fractography. Cleveland: ASM International, 1987. p. 34-63. DOI: https://doi.org/10.31399/asm.hb.v12.a0001831.

KUMAR, S.; SINGH, D.; KALSI, N. S. Analysis of surface roughness during machining of hardened AISI 4340 steel using minimum quantity lubrication. **Materials Today: Proceedings**, v. 4, n. 2, Part A, p. 3627-3635, 2017. DOI: https://doi.org/10.1016/j.matpr.2017.02.255.

LEE, G. M.; LEE, J. U.; PARK, S. H. Effects of surface roughness on bending properties of rolled AZ31 alloy. **Journal of Magnesium and Alloys**, v. 11, n. 4, p. 1224-1235, 2023. DOI: https://doi.org/10.1016/j.jma.2021.11.029.

LI, M.; ZHAO, W.; LI, L.; HE, N.; STEPAN, G. Influence of milling stability on machined surface integrity and fatigue performance of Ti-6Al-4V titanium alloy. **Engineering Failure Analysis**, v. 168, 109103, 2025. DOI: https://doi.org/10.1016/j.engfailanal.2024.109103.

LI, W.; GUO, Y.; GUO, C. Superior surface integrity by sustainable dry hard milling and impact on fatigue. **CIRP Annals**, v. 62, n. 1, p. 567-570, 2013. DOI: https://doi.org/10.1016/j.cirp.2013.03.024.

LI, X.; GUAN, C.; ZHAO, P. Influences of milling and grinding on machined surface roughness and fatigue behavior of GH4169 superalloy workpieces. **Chinese Journal of Aeronautics**, v. 31, n. 6, p. 1399-1405, 2018. DOI: https://doi.org/10.1016/j.cja.2017.07.013.

LIANG, X.; LIU, Z.; WANG, B. State-of-the-art of surface integrity induced by tool wear effects in machining process of titanium and nickel alloys: a review. **Measurement**, v. 132, p. 150-181, 2019. DOI: https://doi.org/10.1016/j.measurement.2018.09.045.

LIU, H.; SCHRAKNEPPER, D.; BERGS, T. Investigation of residual stresses and workpiece distortion during high-feed milling of slender stainless steel components. **Procedia CIRP**, v. 108, p. 495-500, 2022. DOI: https://doi.org/10.1016/j.procir.2022.03.077.

LU, X.; JIA, Z.; WANG, H.; FENG, Y.; LIANG, S. Y. The effect of cutting parameters on micro-hardness and the prediction of Vickers hardness based on a response surface methodology for micro-milling Inconel 718. **Measurement**, v. 140 p. 56-62, 2019. DOI: https://doi.org/10.1016/j.measurement.2019.03.037.

MOLCHANOV, L. N. Fractures and fracture energy of alloy steels are subject to static, impact, and repeated impact bending. **Strength of Materials**, v. 8, p. 651-655, 1976. DOI: https://doi.org/10.1007/BF01528123.

MÜNSTERMANN, S.; WECHSUWANMANEE, P.; LIU, W.; LIAN, J. Surface roughness influences on localization and damage during forming of DP1000 sheet steel. **Procedia Manufacturing**, v. 29, p. 504-511, 2019. DOI: https://doi.org/10.1016/j.promfg.2019.02.168.

NGUYEN, T.-T. Prediction and optimization of machining energy, surface roughness, and production rate in SKD61 milling. **Measurement**, v. 136, p. 525-544, 2019. DOI: https://doi.org/10.1016/j.measurement.2019.01.009.

PATEL, V. D.; GANDHI, A. H. Analysis and modeling of surface roughness based on cutting parameters and tool nose radius in turning of AISI D2 steel using CBN tool. **Measurement**, v. 138, p. 34-38, 2019. DOI: https://doi.org/10.1016/j.measurement.2019.01.077.

PEREIRA, J. C. C.; RODRIGUES, P. C. M.; ABRÃO, A. M. The surface integrity of AISI 1010 and AISI 4340 steels subjected to face milling. **Journal of the Brazilian Society of Mechanical Sciences and Engineering**, v. 39, p. 4069-4080, 2017. DOI: https://doi.org/10.1007/s40430-017-0870-1.

PEREZ, I.; MADARIAGA, A.; CUESTA, M.; GARAY, A.; ARRAZOLA, P. J.; RUIZ, J. J.; RUBIO, F. J.; SANCHEZ, R. Effect of cutting speed on the surface integrity of face milled 7050-T7451 aluminum workpieces. **Procedia CIRP**, v. 71, p. 460-465, 2018. DOI: https://doi.org/10.1016/j.procir.2018.05.034.

SALES, W. F.; SCHOOP, J.; SILVA, L. R. R.; MACHADO, Á. R.; JAWAHIR, I. S. A review of surface integrity in machining of hardened steels. **Journal of Manufacturing Processes**, v. 58, p 136-162, 2020. DOI: https://doi.org/10.1016/j.jmapro.2020.07.040.

SINGH, J.; KIM, M.-S.; CHOI, S.-H. The effect of initial texture on micromechanical deformation behaviors in Mg alloys under a mini-V-bending test. **International Journal of Plasticity**, v. 117. p. 33-57, 2019. DOI: https://doi.org/10.1016/j.ijplas.2018.01.008.

TAN, L.; YAO, C.; ZHANG, D.; REN, J.; ZHOU, Z.; ZHANG, J. Evolution of surface integrity and fatigue properties after milling, polishing, and shot peening

of TC17 alloy blades. **International Journal of Fatigue**, v. 136, 105630, 2020. DOI: https://doi.org/10.1016/j.ijfatigue.2020.105630.

TOMADI, S. H.; GHANI, J. A.; HARON, C. H. C.; AYU, H. M.; DAUD, R. Effect of cutting parameters on surface roughness in end milling of AlSi/AlN metal matrix composite. **Procedia Engineering**, v. 184, p. 58-69, 2017. DOI: https://doi.org/10.1016/j.proeng.2017.04.071.

WECHSUWANMANEE, P.; LIAN, J.; SHEN, F.; MÜNSTERMANN, S. Influence of surface roughness on cold formability in bending processes: a multiscale modeling approach with the hybrid damage mechanics model. **International Journal of Material Forming**, v. 14, p. 235-248, 2021. DOI: https://doi.org/10.1007/s12289-020-01576-7.

WILLIANS, J. A.; DWYER-JOYCE, R. S. Contact between solid surfaces. *In*: BHUSHAN, B. (ed.). **Modern tribology handbook**. Boca Raton: CRC Press, 2001. p. 121-162.

ZHAO, Y.; GONG, B.; LIU, Y.; ZHANG, W.; DENG, C. Fatigue behaviors of ultrasonic surface rolling processed AISI 1045: The role of residual stress and gradient microstructure. **International Journal of Fatigue**, v. 178, 107993, 2024. DOI: https://doi.org/10.1016/j.ijfatigue.2023.107993.

ZHENG, G.; CHENG, X.; DONG, Y.; LIU, H.; YU, Y. Surface integrity evaluation of high-strength steel with a TiCN-NbC composite coated tool by dry milling. **Measurement**, v. 166, 108204, 2020. DOI: https://doi.org/10.1016/j.measurement.2020.108204.

ZHOU, J.; QI, Q.; LIU, Q.; WANG, Z.; REN, J. Determining residual stress profile induced by end milling from measured thin plate deformation. **Thin-Walled Structures**, v. 200, 111862, 2024. DOI: https://doi.org/10.1016/j.tws.2024.111862.